6.1.2 Nanowire microarray arrays

The method described in the previous section (6.1.1) is very suitable for the production of numerous small arrays. Using the appropriate mask for template fabrication large quantities can be obtained. Figure 6.5a depicts an optical microscopy image of an array of 19x25 microarrays embedded in a polymer membrane. With the depicted density more than 5000 arrays can be grown in 1 cm^2. In Figure 6.5b a similar array is shown after template removal.

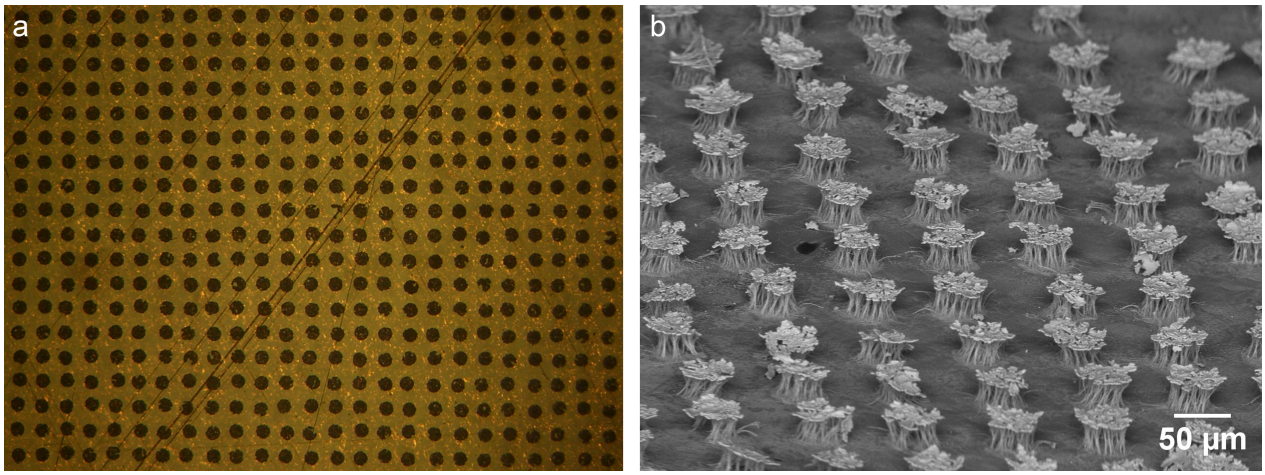

Figure 6.5: Images of nanowire microarray arrays. (a) Top view on microarrays embedded in a polymer membrane. The arrays shown as dark spots measure 50 μm in diameter. (b) FESEM analysis of microarrays connected to the cathode layer.

6.2 3-D nanowire networks

In this section, the direct synthesis of highly-ordered large-area nanowire networks by a hard-template based method using electrodeposition within nanochannels of track-etched polymer membranes is reported. Control over the complexity of the networks and the dimensions of the integrated nanostructures are achieved by a modified template fabrication. The networks exhibit high surface area and excellent transport properties turning them into a promising electrocatalyst material as demonstrated by cyclic voltammetry studies on platinum nanowire networks catalyzing methanol oxidation. The method opens up a new general route for interconnecting nanowires to stable macroscopic network structures of very high integration level that allow easy handling of nanowires while maintaining their connectivity.

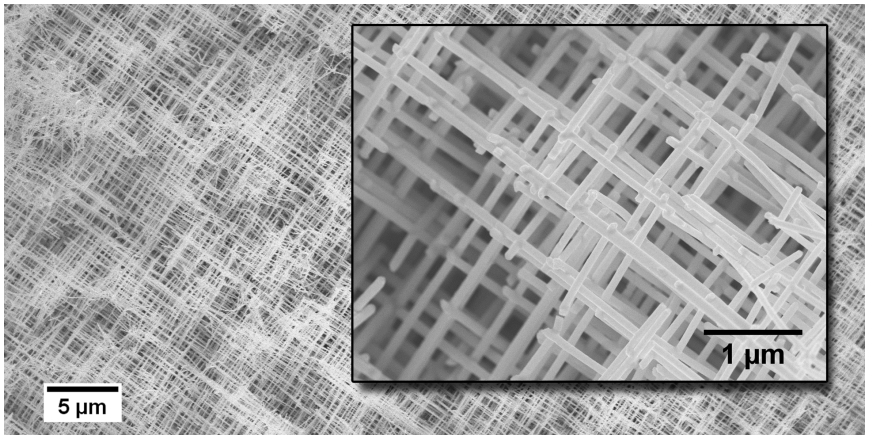

Figure 6.6: FESEM image showing a continuously organized 3-D architecture of interconnected platinum nanowires. The arrangement can be described as an open porous network structure exhibiting meso- and macropores.

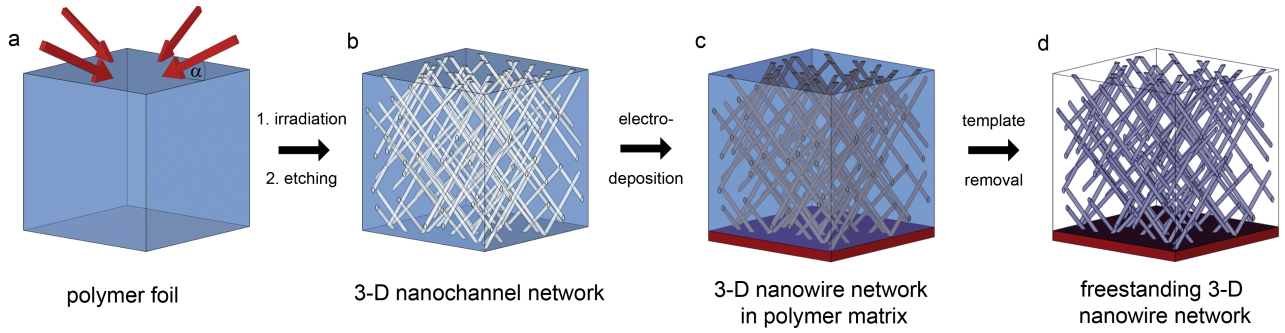

Figure 6.7: Schematic showing the template fabrication and the formation of a 3-D nanowire network: A polymer membrane (a) is irradiated in several steps from different directions. Subsequent etching leads to the formation of a 3-D nanochannel network (b) that can be filled with the desired material. After removing the polymer matrix from the embedded nanowire network (c), a freestanding 3-D nanowire network (d) is obtained.

6.2.1 Fabrication

The basic concept of the approach relies on the ion-track template electrodeposition method that was used to grow arrays of parallel aligned nanowires with excellent control over the wire morphology and crystallinity.[14,17] Starting from this conventional fabrication technique, the method was extended to organize nanowires into more complex structures by changing the template fabrication process. The main steps of NWN production are schematically shown in Figure 6.7. In brief, a polymer membrane is through-irradiated systematically with energetic heavy ions in several steps (each from different direction at an incident angle α with respect to the surface of the polymer) in such a way as to enable crossing of the ion tracks. Subsequent chemical etching of the tracks to nanochannels with the desired diameter leads to the formation of a 2-D or 3-D nanochannel network, serving as a template. By electrochemical deposition of the chosen material into the nanochannels, the shape of the template is adopted, and thus well-defined interconnected nanowires are created. Afterwards, the arising network structure can be liberated from the template material by an organic solvent, resulting in freestanding nanowire networks. According to the requirements, the metal layer, which served as a cathode for nanowire deposition, can be removed.
Note that two steps of the production process are decisive with regard to the overall structure: (i) the irradiation step defines the integration density and the absolute and relative orientations of the nanowires, and (ii) the electrochemical deposition process has a strong influence on the composition and crystal structure of the nanowires.
Here, Pt structures are fabricated to exemplify that the combination of specifically designed template materials, featuring controlled arrangements of nanochannels, with electrochemical deposition is suitable to produce highly ordered nanowire networks. Eventually, other materials are used to prove the method's general applicability.

6.2.2 Structural characterization

Structure and stability

Figure 6.8 shows representative images of Pt nanowire networks. The optical images prove that the networks exist as macroscopic objects without the need for a support. A typical network sample is de-

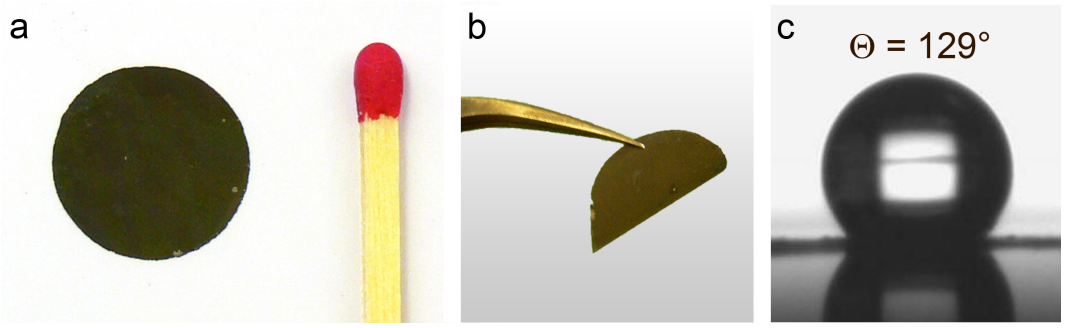

Figure 6.8: Optical images of a nanowire network: (a) A freestanding Pt network with dimensions on the macroscale. (b) The robust network structure can be manipulated with tweezers. (c) Water contact angle measurement of a Pt NWN.

picted in Figure 6.8a with lateral dimensions of more than 1 cm^2 and 30 µm in thickness. Due to the high mechanical stability, the freestanding NWNs can easily be handled and manipulated by tweezers (Figure 6.8b). The assemblies allow the investigation of macroscopic effects like the wettability (Figure 6.8c). Pt NWNs are very hydrophobic with a water contact angle of 129°, which was measured by a video contact angle instrument.

Characterization by field-emission scanning electron microscopy (Figure 6.9) reveals that the surface of the Pt network structure shown in Figure 6.9a appears homogeneous at low magnification; individual nanowires, creating an open porous network, can be identified at higher magnification (inset of Figure 6.9a). The 1-D building blocks are directly connected to each other by junctions consisting of material, which is an inherent part of each crossing nanowire forming a metallic bond. Consequently, the wires act not only as functional elements but also as interconnects. These stable connections can be observed in Figure 6.9b-c. Several cross-junctions, representing a fundamental kind of interconnection that is necessary for complex network structures, are visible. The mechanical stability depends strongly on nanowire diameter, network dimensions, and degree of cross-linking. As demonstrated by imaging a cross-sectional area in Figure 6.9d, even thin networks, consisting of nanowires with an average diameter of only 35 nm, are stable, if the integration density is sufficiently high.

The method allows adjusting the diameter, length, orientation, integration level and degree of connectivity of the nanowires at once. Thereby, the network porosity of the network can be tuned covering a wide range. No other existing method can achieve all this together. Using this approach, continuously connected structures with lateral size of several square centimeters and up to 60 µm in height could readily be synthesized. The fundamental limits of the approach in terms of template dimensions are defined by the projected ion range in the template material, which depends on the ion species and irradiation conditions (as described in 2.1.1). In the case of heavy ions like Au with E=10 MeV/u, the template cannot be much thicker than 100 µm if the angle of incidence α=45°. The smallest nanochannel that can be achieved in polycarbonate is ≈10 nm. However, due to the etching process it is not possible to obtain nanochannles of cylindrical geometry for an aspect ratio of diameter to length, which is larger than approximately 1:1000. The networks with the highest integration level in this work consisted of more than 1×10^{13} NWs/cm^3 and a by multiples higher number of branching points. Increasingly complex structures arise with the number of integrated nanowires, leading to intensified interwire communication and the creation of new functionalities. These structures, consisting only of nanowires, provide the excellent capability to investigate how different combinations of nanowires act in comparison to individual nanowires.

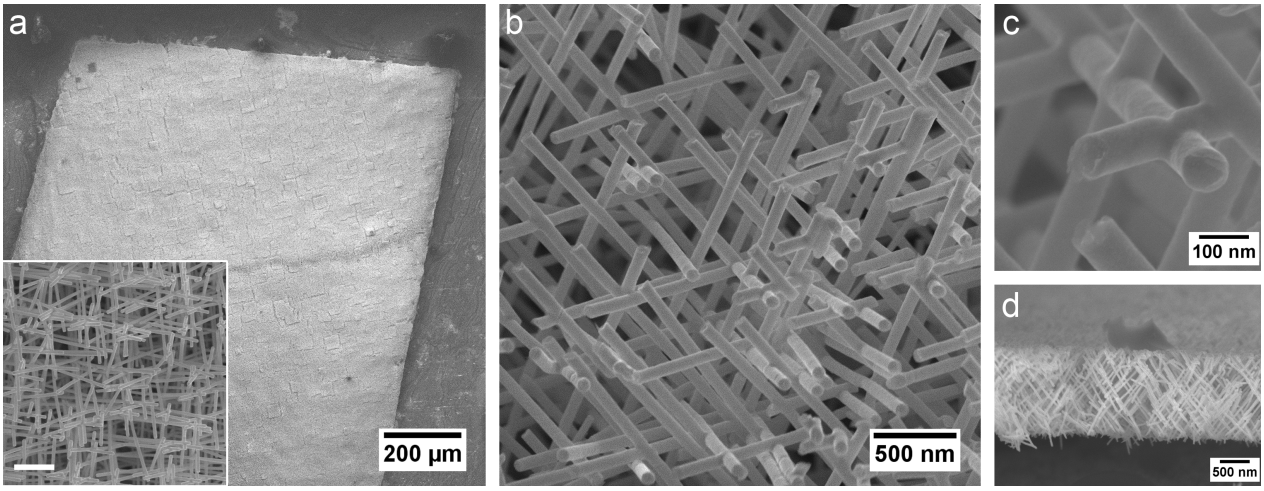

Figure 6.9: FESEM images of Pt nanowire networks. (a) Low magnification image of a piece cut from a larger NWN. The inset shows an area with higher magnification. Inset scale bar is 1 μm. (b) Interconnected nanowires of a network. (c) Junctions of 1-D building blocks, illustrating the connectivity, are clearly highlighted. (d) Cross-section of a thin and mechanical stable NWN (average nanowire diameter is 35 nm).

Branching geometry of network nanowires

The branching geometries are determined by the irradiation protocol, which had been applied during the template fabrication process. Adjusting the total number of irradiation steps, and the angle and the direction, from which the heavy ions hit the polymer membrane during each irradiation step, allows precise control over the branching geometries. The formation of a simple cross-junction, needed for a 2-D network, requires two irradiation steps. More complex branching geometries are obtained by irradiating repeatedly. Panels a and b of Figure 6.10 display NWNs in whose production 4 and 8 irradiations, respectively, were involved. From these images, the different growth directions of the wires, indicated by sketched in arrows, can be observed. Furthermore, the number of potential nanowires crossing in one junction may be derived. The anisotropy induced by the growth directions is also evident in nanowire arrangements that were disconnected from the total network probably due to imposed mechanical stress (Figure 6.10c). Assemblies originating from networks that were grown in templates, irradiated in 4

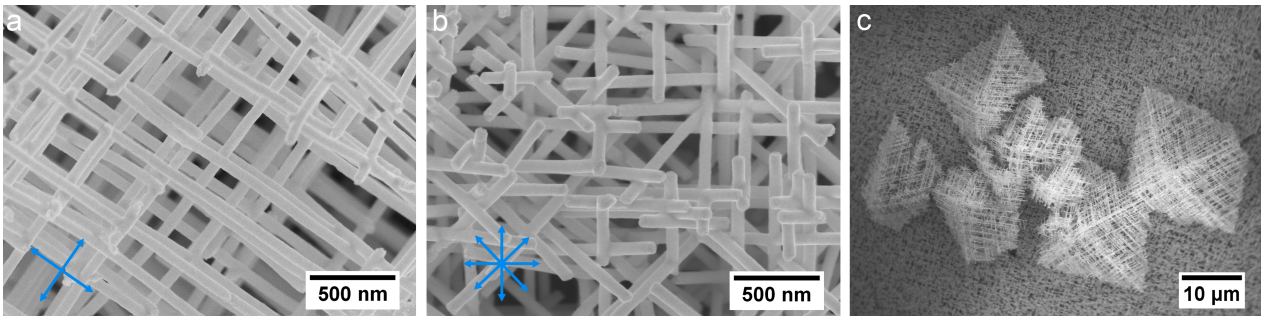

Figure 6.10: FESEM images of Pt nanowire networks. (a, b) Differently oriented nanowires demonstrating specifically generated branching geometries. Arrows correspond to the growth directions of the wires. The network templates have been irradiated from 4 and 8 directions, respectively. (c) Highly ordered nanowire assemblies that were disconnected from the network maintain the orientation of the wires.

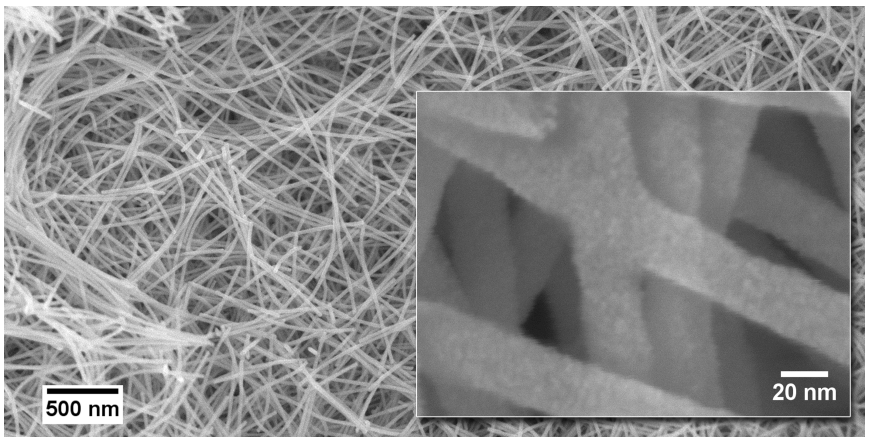

Figure 6.11: FESEM image of a NWN consisting of nanowires with an average diameter of 20 nm. The wires lost the orientation after template removal, but are still interconnected. The inset depicts the network at higher magnification.

evenly distributed directions with α=45°, are often organized to octahedrons (Supporting information, Figure S6).

It is noteworthy that no individual nanowires are found that leave the network. This aspect is important regarding safety issues, since separated nanowires can be internalized by living cells, whereat they may have toxic effects.[169]

However, networks consisting of nanowires with a small average diameter and with relative low integration density, such as the NWN depicted in Figure 6.11, composed of nanowires with an average diameter of 20 nm, cannot maintain the orientation given by the template. The nanowires bend, but are still connected to a macroscopic object, as which they can be manipulated (Supporting information, Figure S7).

Furthermore, investigations by FESEM reveal well-defined nanowires of cylindrical geometry. The Pt network nanowires that were produced by dc deposition show a very smooth surface. The diameter distribution of the wires is smaller than 10% for all regarded samples revealing an excellent quality of the used templates. For network nanowires with decreasing average diameter the standard deviation slightly increases. In addition, it was observed that thinner templates result in nanowires with smaller scatter in nanowire diameter. These findings are in agreement with reports about nanowire arrays grown in polycarbonate templates with parallel aligned nanochannels.[140,170] A typical Pt nanowire network with an average nanowire diameter of 29.9 nm that was fabricated in a 10 µm thick template has a standard deviation of 2.0 nm (7%). A histogramm illustrating the diameter distribution is given in Figure S8 (Supporting Information).

Images of NWNs obtained by transmission electron microscopy exemplify not only the precise replication of the template shape but also show particularly well how nanowires are interconnected. A representative micrograph of an isolated node taken from the edge of a nanowire network is depicted in Figure 6.12a. The network nanowires exhibit an average diameter of 13 nm. At higher magnification, individual grains of the polycrystalline nanowires can be identified (Figure 6.12b). The randomly oriented face-centered cubic Pt crystallites have an average size of <5 nm. Very small grains are typical of nanowires that consist of a metal with high melting point and follow a 3-D nucleation-coalescence growth mechanism.[66] Nanoscale structural features are consistent with broadenings of the 111, 200, 220, and 311 reflexes in X-ray diffractograms (Supporting Information, Figure S9). A representative selected area electron diffraction (SAED) pattern, shown in the inset of Figure 6.12b, additionally indicates the polycrystalline structure of the nanowires.

6.2.3 Composition

Studies were conducted on platinum, but it is also demonstrated that a general method was developed by producing NWNs consisting of different metals and semiconductor nanowires.

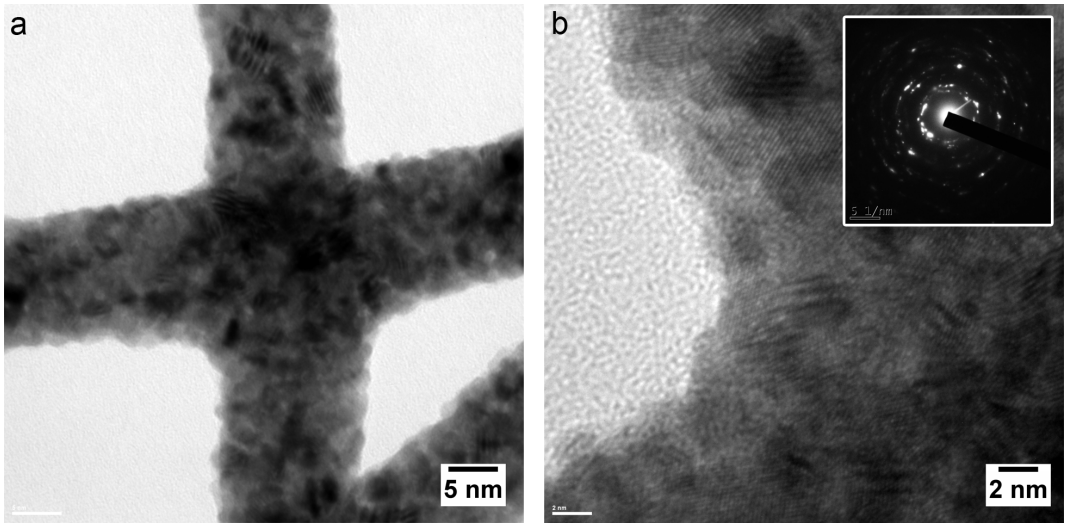

Figure 6.12: TEM images taken from the edge of a Pt NWN: (a) Junction of two crossing nanowires. (b) HRTEM image presenting grains of the polycrystalline wires. The inset shows a representative SAED pattern.

Nanowire networks consisting of Au were fabricated using two methods reported previously for nanowire array fabrication.[17,171] In brief, Au was deposited (i) from a ammonium sulfite gold(I) bath applying a potential of −0.8 V at 50 °C and (ii) from a potassium dicyanoaurate(I) electrolyte at a voltage of −1.3 V at 70 °C. Both synthesis routes were performed under potentiostatic conditions. Imaged by SEM, the Au nanowire networks appear very similar to the Pt NWNs. Although macroscopically interconnected and highly ordered Au assemblies were produced, the mechanical stability is smaller than for the Pt structures resulting in a reduced robustness. As a consequence wires often break if the network is manipulated. Accountable for the reduced mechanical stability of Au nanowire assemblies may be material-specific properties, such as the ductility, but also the crystalline structure, e. g. the crystallite size, which is much larger for the Au nanostructures.

CdTe nanowire networks were produced adopting an electrodeposition protocol from a work of Ohgai et al., who synthesized CdTe semiconductor nanowire arrays using template electrodeposition into AAO templates.[141] CdTe nanowires have been frequently synthesized by template electrodeposition.[172] Here, networks were deposited from an aqueous electrolyte containing 0.1 mol/L $CdSO_4 \cdot 8\ H_2O$, 0.01 mol/L TeO_2, and 1 mol/L H_2SO_4 under potentiostatic conditions applying −0.5 V at 0 °C.
Since the obtained CdTe nanowire networks also appear similar using SEI, energy dispersive X-ray (EDX) analysis was employed to monitor the composition. SEM images and EDX spectra for Pt, Au, and CdTe NWNs are presented in the appendix (Supporting Information, Figures S10-S12).

Within the thesis only a few different materials were exemplarily synthesized to prove the general applicability of the method. However, it is indicated that for the selection of the templates, as well as the network materials, the wide range reported for electrodeposited nanowire arrays by the template method can be used, including metals, semiconductors, and composite materials, with the same excellent control over the composition.[12,173]

6.2.4 Cap formation

The growth of caps forming on top of nanowire networks, which reached the end of the nanochannels, is different from cap formation on parallel aligned nanochannels. Since the nanochannels are interconnected and show a high degree of orientation inside the network templates, the process can not be regarded as independent growth. While individual caps forming on nanochannel arrays have

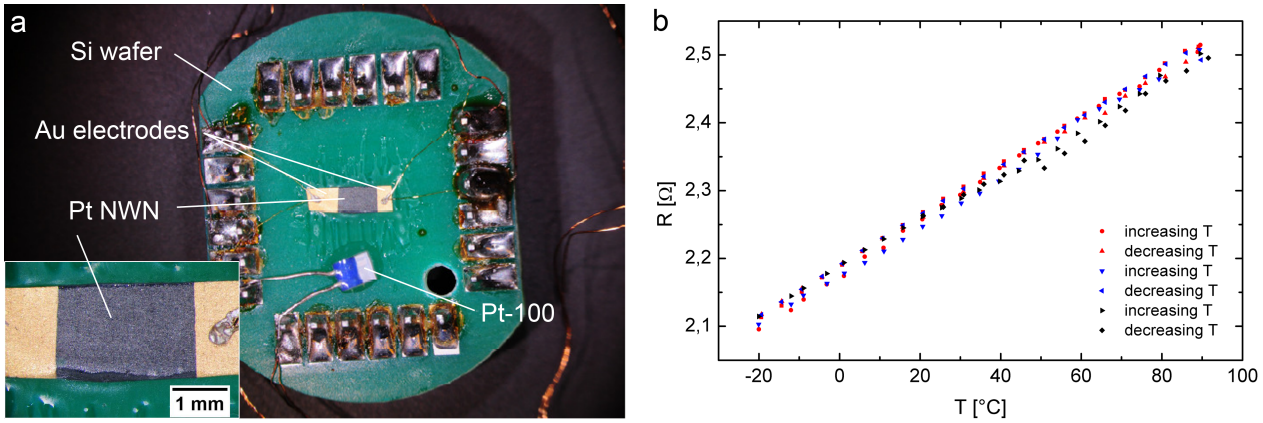

Figure 6.13: Investigation of electrical transport properties of a NWN consisting of 60 nm diameter nanowires. (a) Experimental setup showing the contacted NWN on a silicon wafer. The inset depicts the NWN at higher magnification. (b) Electrical resistivity *R* versus the temperature *T*.

a hemispherical shape, isolated growth on channel openings is not observed in the case of nanowire networks.

The interaction becomes more pronounced as the integration density, and hence the number of branching points increases. The orientation induced by the irradiation is evident in the cap geometry. Caps grown on a nanowire network, whose template had been irradiated in 4 evenly distributed directions with α=45°, are organized into squares. Template irradiation from 8 evenly distributed directions results in caps forming octahedrons. Microscopy images of cap geometries grown on different nanowire assemblies can be found in the appendix (Supporting information, Figure S13).

6.2.5 Transport properties

For the measurement of the electrical transport properties, a Pt NWN network was synthesized and contacted with electrodes as described in section 4.2 (page 39). Measurements were performed by H. Reith at the University of Applied Sciences (Rüsselsheim). Figure 6.13a shows a picture of the experimental setup. In the inset, the measured network area (2.4x1.7 mm^2), which appears gray, can be identified between two Au covered network areas. The network consists of nanowires with an average diameter of 60 nm and a integration density of 1.4x10^9 wires/cm^2. The template had been irradiated in 4 evenly distributed directions with α=45°.

Investigation of the resistivity *R* at room temperature reveals a value of ≈2.2 Ω that is constant within the measured time period of 5000 s (Supporting information, Figure S14a). Figure 6.13b shows several measurements of the resistivity as a function of the temperature *T* ranging from -20 to 100 °C. The average temperature coefficient of the electrical resistivity β of the nanowire network is 1.6x10^{-3} K^{-1} (Supporting information, Figure S14b). This decrease by a factor of 2.44 in comparison to the Pt bulk value of β_0=3.9x10^{-3} K^{-1} at room temperature is in good agreement with measurements on single Pt nanowires.[45]

It has been demonstrated for thin films that the ratio of the electrical conductivity σ and the TCR β is the same as that of the corresponding bulk values σ_0 and β_0.[174] With the equation

$$\frac{\beta_{nw}}{\beta_0} \approx \frac{\rho_0}{\rho_{nw}} \tag{6.1}$$

the specific resistivity of a nanowire ρ_{nw}=2.7x10^{-7} Ωm was estimated. The total resistivity of the network R_t is composed of the resistivities of all components R_n that are connected in parallel according to equation 6.2:

$$\sum_{n=1}^{N} \frac{1}{R_n} = \frac{1}{R_t} \tag{6.2}$$

R_n can be calculated with the effective length of interconnected nanowires L_{nw} (= 2.4 mm · $\sqrt{2}$) and ρ_{nw}:

$$R_n = \frac{\rho_{nw} L_{nw}}{\pi r^2} = 324114\ \Omega \tag{6.3}$$

Consequently, the number of interconnected nanowires N=147 324. In consideration of the nanowire density and the network dimensions, this value indicates that each nanowire is connected with several other nanowires.

6.2.6 Electrochemical investigations

Since all nanowires of a network are interconnected, excellent transport properties exist. Electronic continuity was also probed using cyclic voltammetry. Cyclic voltammograms of Pt NWNs were recorded in nitrogen purged 0.5 mol/L H_2SO_4 solution at a scan rate of 50 mV/s between 0 and 1.3 V with respect to the reversible hydrogen electrode (RHE). The samples had been washed extensively in dichloromethane, ethanol, 1 mol/L NaOH solution, and water to remove impurities. Figure 6.14 shows representative CV curves of a sample being contacted on an Au wire and of the pristine Au wire electrode. It was found that standard hydrogen adsorption/desorption features known for polycrystalline Pt appear in the 0-0.4 V region. The peaks are consistent with literature reports and indicate the presence of {111}, {110}, and {100} crystal faces.[129,175,176] Contributions from the double layer charging to the current are only small. For the pristine Au wire, no distinct adsorption/desorption features were observed in the base voltammogram.

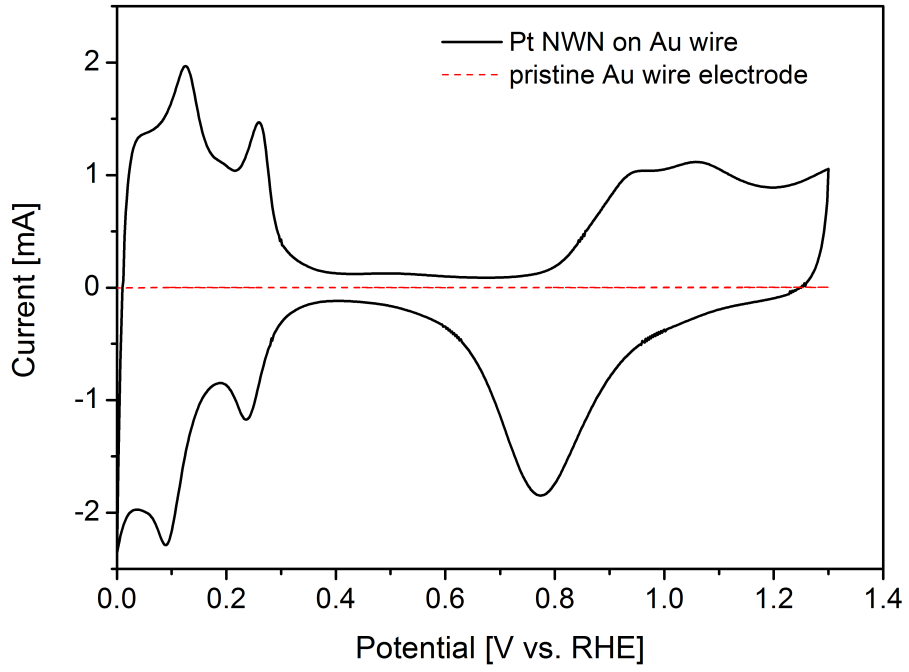

Figure 6.14: Electrochemical characterization of Pt NWNs: Cyclic voltammetry of a Pt NWN on a gold wire (solid line) and a pristine gold wire electrode (dashed red line) performed in 0.5 mol/L H_2SO_4 at a scan rate of 50 mV/s.

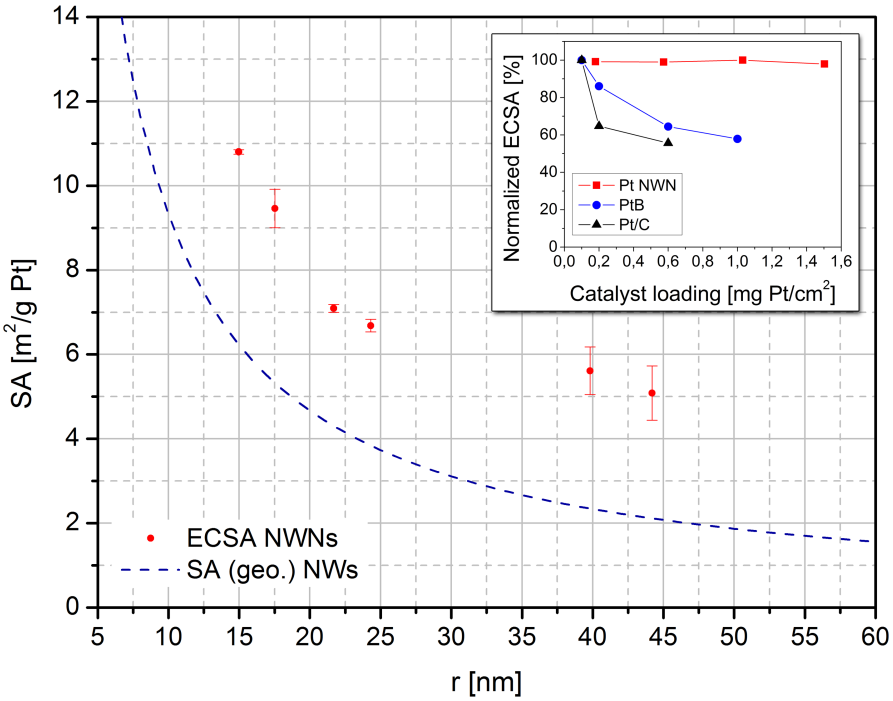

Figure 6.15: Electrochemically active surface area of Pt NWNs versus average nanowire radius. The dashed line represents the theoretical surface area of Pt nanowires calculated using a simple cylinder model. In the inset, the decrease of ECSA with catalyst loading for Pt NWNs, PtB, and Pt/C is shown

Surface area

The electrochemically active surface area (ECSA) was estimated based on the integrated hydrogen desorption charge $Q_{H,d}$ by means of equation 4.4 as it has been frequently used in previous reports.[136,143–145] In Figure 6.15a the ECSA of different NWNs is plotted versus the average diameter of the network nanowires. The dashed line represents the geometrical surface area of unconnected Pt nanowires, calculated assuming a cylindrical geometry. A clear connection between the ECSA and the radius can be identified. The obtained NWNs consisting of the thinnest NWs with an average radius r = 15.0 ± 1.0 nm exhibited an ECSA of 10.8 m^2/g Pt. Exact values of the ECSA of all NWNS are given in Table 6.1.
It has to be considered that to maintain the stability of the networks sufficiently high, the integration level of NWNs was adjusted with the wire radius ranging from 1.4x10^9 NWs/cm^2 for r = 44.2 nm to 1.4x10^{10} NWs/cm^2 for r = 15.0 nm. By stepwise increasing the integration level, the point of intersection density rises and the porosity decreases until the total volume of void-space inside the network is finally filled. In this context, the slight decrease in the ratio of the ECSA of the networks to the calculated geometrical SA towards reduced radii, observed in Figure 6.15a, can be explained by the fact that reduced diameters are accompanied by a higher integration level in this study.

To compare the results on NWNs to commercially available state-of-the-art Pt catalysts, CV measurements were performed on glassy carbon electrodes loaded with Pt nanoparticles (PtB, Alfa Aesar) and carbon-supported Pt nanoparticles (Pt/C, 20 wt. % Pt on Vulcan XC-72R, Alfa Aesar). Additional information about the nanoparticle catalyst electrodes are given in section 4.2. The results presented in the inset of Figure 6.15b clearly demonstrate a strong dependence of the ECSA of nanoparticles on the catalyst loading. The highest absolute values of 88.8 m^2/g Pt for Pt/C and 21.2 m^2/g Pt for PtB were achieved with the lowest investigated loadings of 0.1 mg Pt/cm^2. Higher loadings lead to a dramatic de-

Table 6.1: ECSA of NWNs with different average nanowire radius.

r [nm]	NWN mass [μg]	$Q_{H,d}$ [mC]	ECSA [m^2/g Pt]	Error [m^2/g Pt]
44.2	335	3.6	4.6	0.65
39.8	462	5.4	5.6	0.57
24.3	90	1.3	6.7	0.15
21.7	528	7.9	7.1	0.09
17.5	288	5.7	9.5	0.46
15.0	414	9.4	10.8	0.05

crease in active surface area.[144] In the case of Pt NWNs, the ECSA is not affected by the catalyst loading providing always a reasonably high value, besides their relatively large overall dimensions. For Pt NWNs consisting of nanowires with r = 17.5 nm the ECSA is invariably 9.5 ± 0.3 m^2/g Pt within the considered range. The observed trends are a consequence of the varying fraction of loaded platinum being active. As the catalyst loading is increased, the electrode thickness grows, and thus nanoparticle aggregation and loss of electrical contact occur. These two mechanisms, mainly responsible for reduction of the ECSA, cannot be applied to NWNs that were *ab initio* designed as scalable 3-D assemblies. While the thickness of the network is increased to obtain a higher loading, the relative orientation of the nanoscale building blocks is maintained. The porosity of the monolithic structure remains constant and no aggregation is observed. In addition, electrical contact of each nanowire in the network is assured due to the high density of branching points. Note that, in contrast to nanoparticle catalysts, much higher loadings can be achieved for the NWNs without the need for a support material or coating. The thickness of the NWNs is limited by the template, but several networks can be stacked to achieve even thicker catalyst layers. Moreover, it is easily possible to recover the networks from solution and contact them again many times without noticeable loss of ECSA, even though the networks are deformed and compressed during this process. These observations show a remarkable mechanical flexibility and electrical robustness.
The durability of catalyst materials is a related problem that must be addressed to evaluate their applicability. We investigated the degradation by repeated CV in nitrogen-purged 0.5 mol/L H_2SO_4 solution applying a potential of $0 - 1.3$ V with a scan rate of 50 mV/s. Representative curves demonstrating the changes during the durability measurements are shown in Figure 6.16a-c for the different Pt nanomaterials. The developing of the ECSA with number of CV cycles is depicted in Figure 6.16d for all three catalysts. A significant loss of ECSA is observed for PtB and Pt/C, whereas the CV curves show only a slight decrease for Pt NWNs. After 500 cycles the ECSA is reduced about 29 and 43% for PtB and Pt/C, respectively, while the networks have lost only 7% of the ECSA. Responsible for differences in durability are multiple degradation pathways, including the abovementioned mechanisms, which are particle aggregation and loss of electrical contact, and additional effects such as Ostwald ripening and dissolution of platinum followed by migration of Pt ions, which partly do not occur at all in the case of complex nanowire assemblies or are far more pronounced for nanoparticle based catalysts.[143,177]

Electrocatalytic performance

The performance as electrocatalyst for methanol oxidation reaction (MOR) was elucidated by CV in a deareated 0.5 mol/L H_2SO_4 solution containing 0.5 mol/L MeOH at room temperature. Representative CV curves of a Pt NWN, consisting of nanowires with an average radius of 15.0 nm, and of the PtB and Pt/C catalysts are present in Figure 6.17. The curves are normalized by the determined ECSA. The observed features are typical for methanol oxidation catalyzed by Pt nanostructures and are consistent with literature reports.[129,145,178] Peak current densities of the forward anodic peaks (I_f) of Pt NWN, PtB, and Pt/C are 0.76, 0.39, and 0.24 mA/cm^2, respectively, demonstrating the high activity of Pt NWNs.

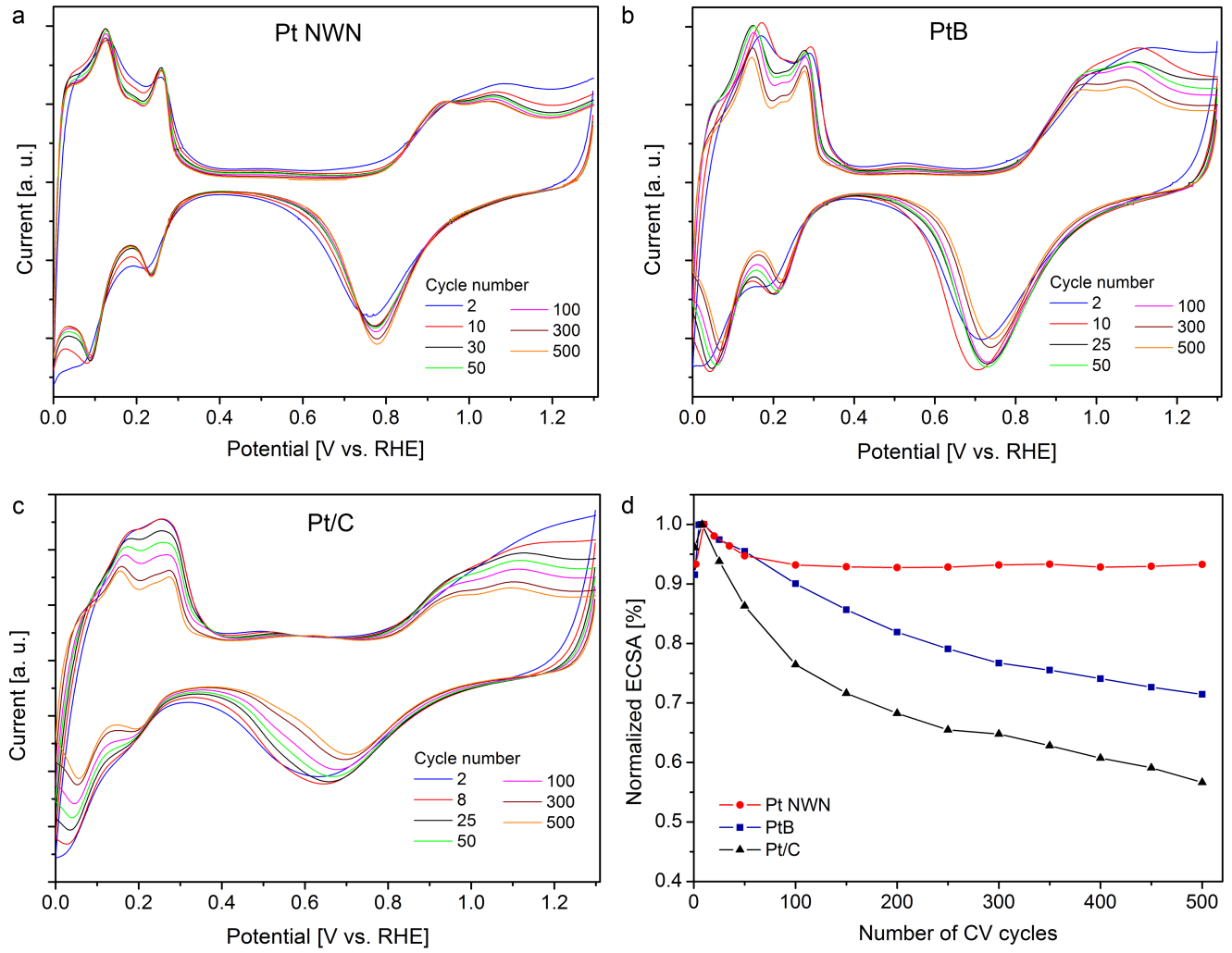

Figure 6.16: (a-c) Representative curves of repeated CV measurements for a Pt NWN, PtB, and Pt/C, respectively, demonstrating changes with number of cycles. (d) Loss of ECSA with number of CV cycles for Pt NWNs, PtB, and Pt/C.

Peak mass activities are 82, 48, and 121 mA/mg Pt for Pt NWNs, PtB, and Pt/C, respectively. The values for the peak current densities and for the mass activities of the different catalysts are shown in the insets of Figure 6.17. Absolute values are specified in Table 6.2. The peak current density of the Pt NWN is more than 3 times higher than that of Pt/C, while the mass activity is still 68% of Pt/C, although the carbon supported catalyst exceeds the NWN manifold in terms of active surface area. In comparison to PtB, Pt NWNs exhibit better performance regarding both current density and mass activity. The commercial catalysts were investigated with a loading of 0.6 and 1.0 mg/cm^2 for Pt/C and PtB, respectively. It has to be carefully considered that the mass activity increases with decreasing loading. For 0.1 mg Pt/cm^2 the mass activities are 0.20 and 0.11 A/mg Pt for Pt/C and PtB, respectively.

As origin for the remarkable electrocatalytic performance of NWNs, following factors may be accountable. First, it is known for 1-D nanostructured electrocatalysts to possess improved electron transport characteristics due to the shape anisotropy of the catalyst material.[142,145,178,179] Compared to nanoparticles, the number of interfaces between the electrocatalysts is reduced for nanowires resulting in larger electronic conductivity. In the case of NWNs, reduction of interfaces is achieved completely, as all nanowires are interconnected providing electronic continuity. Thus, electron transport is carried out solely by the network nanowires and is merely governed by their intrinsic transport properties.[45] In addition, numerous parallel pathways for electron transfer exist throughout the network, since each

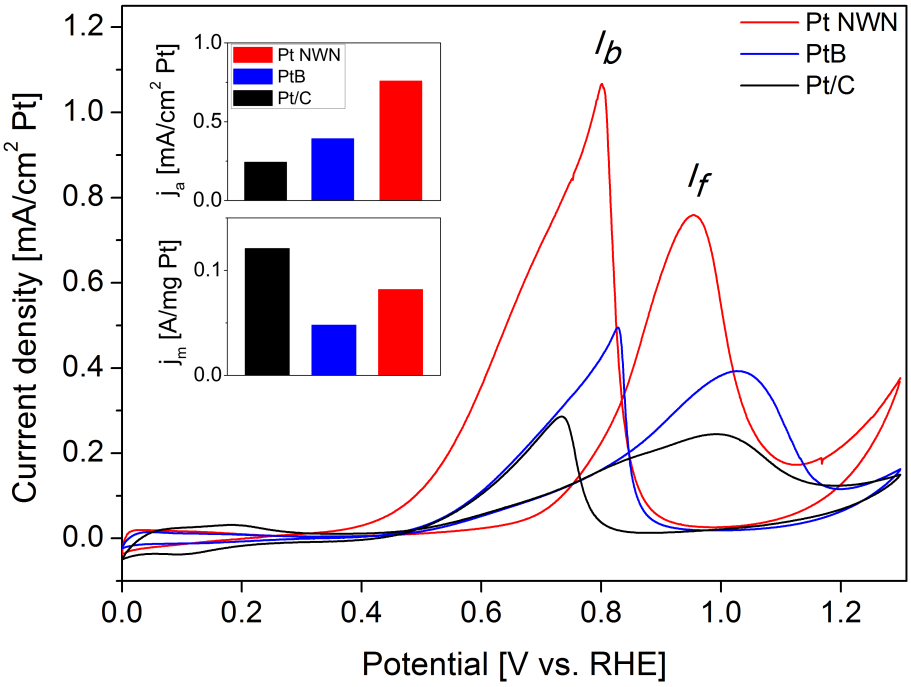

Figure 6.17: CV curves for MOR catalyzed by PtNWN (r=15.0 nm), PtB, and Pt/C in 0.5 mol/L H_2SO_4 + 0.5 mol/L MeOH solution (0-1.3 V, scan rate 50 mV/s). Insets: Peak current densities j_a (top) and peak mass activities j_m (bottom) of the forward anodic peak I_f for Pt NWN, PtB, and Pt/C; I_b is the corresponding backward anodic peak.

Table 6.2: Peak current densities and peak mass activities for NWNs, PtB, and Pt/C.

Catalyst	ECSA [m^2/g Pt]	Current density [mA/cm^2]	Mass activity [mA/mg]
NWN	10.8	0.76	82
PtB	12.2	0.39	48
Pt/C	49.4	0.24	121

nanowire is connected with several other wires. Second, the high porosity in combination with the definitive resistance to agglomeration enables effective exposure of catalytically active sites. In contrast to particle based catalysts, all nanostructures in the NWNs are invariably accessible to reactants through mesopores or even macropores. The porosity can be adjusted in a wide region, ranging from virtually 0% to more than 95%. In this study the porosity of the NWNs was not less than 90%, while the porosity of carbon supports is typically 40-60%.[180] The possibility to tune the accessibility by means of controlling the porosity is very important to be able to compensate for limitations due to mass transport, particularly in the case of electrochemical reactions in solution, or other applications, in which free volume plays a significant role.[94]

On the basis of the peculiar 3-D architecture, the NWNs meet, to an outstanding degree, the requirements for the design of an advanced material for catalysis in terms of conductivity and porosity. However, the specific surface area is significantly lower than for very small Pt nanoparticles. Better catalysts may readily be produced by improving the mass activity alone. This can be achieved by synthesizing Pt alloy based networks or by using network structures of another material as a support for nanoparticle catalysts. The same result may be reached by fabricating porous network nanowires or nanotube networks, but this will also have a strong influence on the mechanical stability of the assembly.